

Constraints on the Higgs-charm coupling by CMS

Andrey Pozdnyakov^{a,*}

^a*Physikalisches Institut III A, RWTH,
Otto-Blumenthal-Strasse, Aachen, Germany*

E-mail: Andrey.Pozdnyakov@cern.ch

The discovery of the Higgs (H) boson ten years ago and successful measurements of its couplings to third generation fermions by ATLAS and CMS experiments mark great milestones for the field of High Energy Physics. The much weaker coupling of the H boson to second generation quarks predicted by the standard model (SM) makes the measurement of the H-charm coupling much more challenging. With the full Run-2 data collected at the LHC a lot of progress has been made by the CMS Collaboration to constrain this coupling. In this report I present the latest results of the direct and indirect measurements of the H-charm coupling by CMS. Direct measurements are performed by searching for the $H \rightarrow c\bar{c}$ decay. It is done in gluon fusion and VH production modes with stronger limits coming from VH mode, $\mu_{VH(H \rightarrow c\bar{c})} < 14.4$ at 95% CL. In the ggH channel the limit is set at $\mu_{ggH(H \rightarrow c\bar{c})} < 45$. Indirect constraints on the charm coupling come from the measurement of the H boson p_T distribution, which leads to a limit of $|\kappa_c| < 35$. A rare H boson decay, $H \rightarrow J/\psi\gamma$, is also searched for at CMS, though giving a limited sensitivity of $\sim 220 \times$ SM. Prospects for future measurements at HL-LHC are also discussed. From the projections it seems feasible to constrain the H-charm coupling better than 2 times the SM value.

*41st International Conference on High Energy physics - ICHEP2022
6-13 July, 2022
Bologna, Italy*

*Speaker

1. Introduction: measurements of the H boson couplings

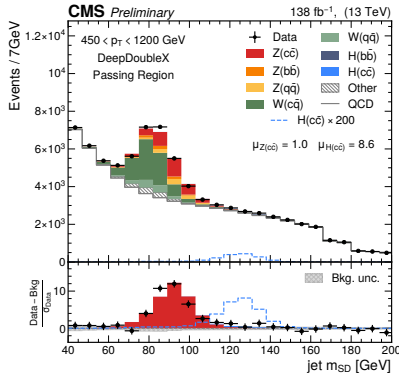
Ten years ago the discovery of the Higgs (H) boson was announced by the ATLAS and CMS Collaborations [1–3], which opened a whole field of study devoted to measuring the properties of the new particle. During the ten years after the discovery a vast number of properties of this particle were measured and so far everything is found to be remarkably consistent with the predictions of the standard model (SM). A few missing pieces are still remaining to be measured. One of them is the H boson coupling to charm quarks. According to the SM, the couplings of the H boson to fermions are proportional to their masses, $y_f \propto m_f$. The coupling of the H boson to the top quark ($m_t = 172$ GeV), bottom quark ($m_b = 4.2$ GeV) and tau lepton ($m_\tau = 1.8$ GeV) have been established by both ATLAS and CMS [4]. Yet to be determined are the couplings to charm ($m_c = 1.3$ GeV), muon ($m_\mu = 0.1$ GeV) and lighter fermions.

An evidence for the $H \rightarrow \mu\mu$ decay with a significance of 3 standard deviations has recently been reported by CMS [5]. In the quark domain the y_b is determined with 15% precision to be consistent with the SM, while y_c has remained to be measured. This report summarizes the searches performed at the CMS experiment [6] to determine the y_c , that were released before July 2022, using the data collected in Run-2 of the LHC operation.

2. Search for $H \rightarrow c\bar{c}$ decay in the gluon fusion production channel

The highest rate of the H boson production at the LHC is through the gluon fusion process, ggH. In June 2022 CMS released a new analysis searching for $H \rightarrow c\bar{c}$ decay in the ggH production mode [7]. Charm quarks from the H boson result in hadronic jets in the final state and this process is extremely difficult to distinguish from multijet production. In order to suppress the multijet background the $H \rightarrow c\bar{c}$ process is searched for in a topology of single high- p_T , large-cone jet (cone parameter $R=0.8$ of the anti-kt algorithm, AK8). Such a large-cone jet contains the product of both charm jets from $H \rightarrow c\bar{c}$ decay. The AK8 jet is required to have large transverse momentum, $p_T > 450$ GeV. This selection reduces multijet background and allows to use a high- p_T jet trigger to collect the events. Furthermore, the H boson candidate jet is tagged with a novel jet flavor tagger, based on a deep neural network (DNN). The model of DNN classifier is made up of convolutional and recurrent units processing low-level inputs. This tagger is described in more detail in Ref. [7]. An optimal working point of the tagger, maximizing the $H \rightarrow c\bar{c}$ expected sensitivity, is chosen, which corresponds to 20.6% signal efficiency and 0.5% multijet efficiency (i.e. 99.5% rejection of light-flavor jets). The corresponding b-flavor efficiency is 12.4%. The tagger allows to distinguish cc, bb, and light flavor jets, thus enabling our search for $H \rightarrow c\bar{c}$.

After a selection of a cc-tagged jet its mass is reconstructed using the “soft-drop” algorithm, which removes the soft and wide-angle radiation from the jet’s constituents. A histogram of the m_{SD} variable is shown in Fig. 1a. Here one can see the falling spectrum of the multijet background (labeled QCD) and a broad peak around 80-90 GeV from the $W \rightarrow qq'$ and $Z \rightarrow q\bar{q}$ processes. There is no peak at 125 GeV from the H boson. Upper limits are set on the H boson production and decay rate in this channel; the limits are obtained from the fit of the m_{SD} distributions to data, in bins of the jet’s p_T . The multijet component is modeled with a polynomial function and the shapes of the W, Z and H processes are obtained from simulation. While no H boson is seen here (as expected from SM), the visible peak from $Z \rightarrow c\bar{c}$ process allows to measure its rate compared



(a)

data-taking year	luminosity, fb ⁻¹	observed (expected) 95% CL upper limit on σ/σ_{SM}
2016	36	413 (210)
2017	42	137 (141)
2018	60	84 (88)
combined	138	45 (38)

(b)

Figure 1: (a) The observed and fitted m_{SD} distributions, combining all p_T categories, and three data taking years. The lower panel shows the residual difference between the model and data, scaled by the statistical uncertainty in the data, effectively showing an approximate significance. Figure from Ref. [7]. (b) Upper limit on ggH production times $H \rightarrow c\bar{c}$ branching fraction, split by data-taking period.

to SM. The measurement yields $r = 0.91 \pm 0.20$. The limit on the H boson production times the $H \rightarrow c\bar{c}$ branching fraction is set to less than 45 times the SM prediction. The results split by the data-taking year are shown in the table of Fig. 1b.

3. Search for $H \rightarrow c\bar{c}$ decay in the VH production channel

The H boson production, associated with a Z or W boson (referred to as vector boson, V) constitutes about 4% of its total production rate in pp collisions at 13 TeV. A search is performed by CMS in VH production channel, with $H \rightarrow c\bar{c}$ and V decaying leptonically [8]. Leptonic decay of the associated vector boson allows to tag an event, independently of the H boson decay, and helps to eliminate the contribution of the multijet background. Leptons make triggering of the detector easier and more efficient (compared to jet triggers used in ggH channel). This allows to select more events in lower- p_T phase space thus increasing signal acceptance. Three channels are studied in the search based on the decay mode of the vector boson: $Z \rightarrow \nu\nu$ (0L channel), $W \rightarrow \ell\nu$ (1L channel) and $Z \rightarrow \ell\ell$ (2L channel), where ℓ denotes muons and electrons.

Two approaches to reconstruct the H boson candidate are used in the analysis, depending on its momentum. The first approach is to consider a large-cone jet aiming for high p_T , boosted, H boson candidates. The cone parameter of $R = 1.5$ of the anti-kt algorithm is used. A novel DNN approach, called ParticleNet [9], is used to tag the jets as cc-candidates. If the p_T of the candidate jet is above 300 GeV, the event is categorized as boosted. Otherwise, a second approach is considered, when two small-cone jets (cone parameter $R = 0.4$) are used as candidates from $H \rightarrow c\bar{c}$ decay. If multiple such jets are reconstructed, the two that have higher probability of the charm tagger are selected. The DeeJet algorithm [10] is used for flavor tagging of the jets in this topology. An event can be categorized either as boosted (1 large-cone jet) or non-boosted (2 small-cone jets).

In the boosted topology the events are divided into signal-like and background-like using a BDT discriminant, illustrated in Fig. 2 (left), with 7-10 kinematic input variables (depending on the V decay channel), excluding the mass of the cc-candidate. The signal-like events with high BDT

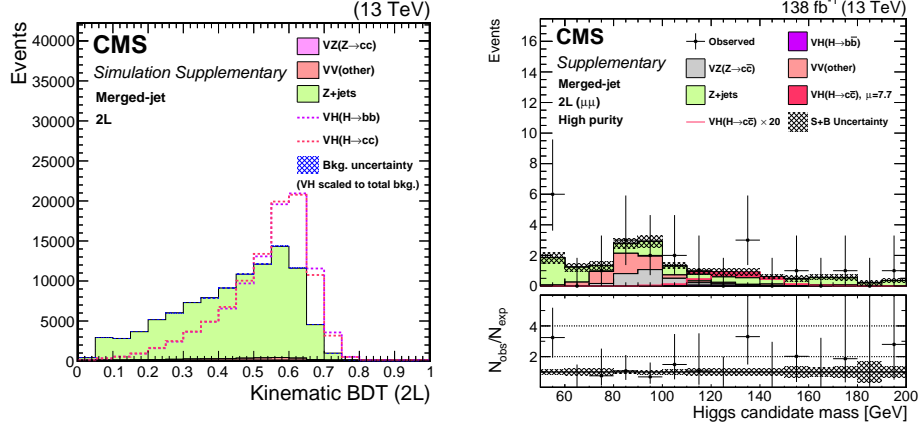


Figure 2: (Left): A BDT distribution in VH(cc) boosted topology in 2L channel. A cut on BDT score value above 0.55 is used to separate signal-like component. Region below 0.55 is used as a control region to constrain backgrounds normalization. (Right): A distribution of the soft-drop mass of the cc-candidate jet, after the final fit to data. Figures from Ref. [8].

score are further subdivided in three categories based on the score of the ParticleNet tagger. Then the soft-drop mass of the cc-candidate jet is used to extract the signal component in each category. The H boson is expected to give a peak at around 125 GeV, while the background has a continuous spectrum. This distribution for the 2L channel in the high purity category is shown in Fig. 2 (right). The shapes of the background processes (Z+jets, W+jets and $t\bar{t}$) are modeled from MC simulation, while their normalization is constrained to data in a control region of low BDT score. To obtain the final limit, a simultaneous fit of the control and signal regions is performed, combining with the fit in 2-jet topology, described below.

In the 2-jet topology a BDT is trained to separate signal and backgrounds using 14-27 input features (depending on V decay channel), including the mass of the H boson candidate and the scores of the DeepJet tagger of both jets. Distributions of the BDT scores in each channel are fit to data in order to extract the signal strength. Control regions are used for constraining the normalization of the major backgrounds: V+jets and $t\bar{t}$. A simultaneous fit of 1-jet and 2-jets topologies results in the 95% CL upper limit on the signal strength, $\mu_{VH(H\rightarrow c\bar{c})} < 14.4$. Detailed results of the expected and observed limits split by channel are shown in Table 1.

The limit on the signal strength can be translated to the limit on the Higgs-charm coupling or, more conveniently, on the coupling modifier, $\kappa_c = y_c/y_c^{SM}$. Assuming all other couplings except

	Combined	boosted (1 jet)	non-boosted (2 jet)	0L	1L	2L
Expected UL on σ/σ_{SM}	7.6	8.8	19.0	12.6	11.5	14.3
Observed UL on σ/σ_{SM}	14.4	16.9	13.9	18.3	19.1	20.4

Table 1: Expected and observed upper limits on VH(cc) process. The results are also shown splitted by the H boson candidate topology and by V boson decay channel.

κ_c have SM values, we use the formula $\mu_{VH}(H \rightarrow c\bar{c}) = \frac{\kappa_c^2}{1+B_{SM}(H \rightarrow c\bar{c}) \times (\kappa_c^2 - 1)}$ and perform likelihood scans to obtain a limit on κ_c . We find that at 95% CL $|\kappa_c|$ lies in the interval [1.1, 5.5], with an expected upper limit of $|\kappa_c| < 3.4$.

As a cross-check to the analysis procedure the $Z \rightarrow c\bar{c}$ process in VZ production channel was studied. From the experimental point of view this process is very similar to VH(cc), except for the mass of the Z(H) boson. The $Z \rightarrow c\bar{c}$ process was observed and its signal strength was measured to be $\mu_{VZ}(Z \rightarrow c\bar{c}) = 1.01 \pm 0.22$, in agreement with the SM expectation, as shown in Fig. 3 (right).

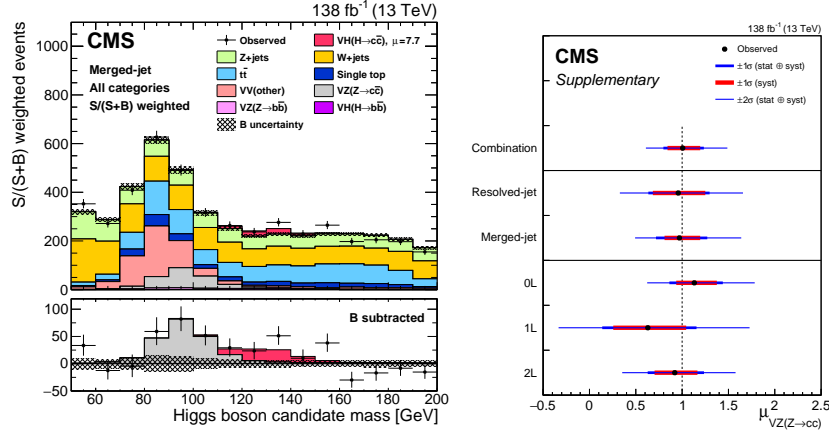


Figure 3: (Left): Mass distribution of the H(Z) boson candidate in VH(cc) analysis; (Right): Signal strength measurement for $Z \rightarrow c\bar{c}$ cross-check analysis, split into three V boson decay channels, and cc-candidate topology. Figures from Ref. [8].

4. Constraints from differential measurements and rare decay $H \rightarrow J/\psi + \gamma$

Differential distributions of the H boson cross section, particularly as a function of p_T^H , are sensitive to the H-charm coupling. The sensitivity comes from ggH production with fermions "running in the loop" of that Feynman diagram. The differential measurements were performed by CMS in $H \rightarrow \gamma\gamma$, $H \rightarrow ZZ$ and $H \rightarrow b\bar{b}$ decay channels [11]. A distribution of p_T^H from these measurements is used in a fit to a signal model with freely floating coupling modifiers κ_b and κ_c . The fit leads to a limit on these couplings as shown in Fig. 6 in Ref. [11]. Only with a partial Run-2 data set this measurement provides a constraint on the H-charm coupling to $|\kappa_c| < 35$.

The rare decay process $H \rightarrow J/\psi\gamma$ is sensitive to the H-charm coupling, as the decay can proceed through a charm quark loop [12]. The branching fraction of this process is very small. Nevertheless, experimentally it is straightforward to look for $J/\psi \rightarrow \mu\mu$ process with an additional photon, and plotting the invariant mass, $m_{\mu\mu\gamma}$, around the expected H boson mass, as it was done in Ref. [12]. It allows to set an upper limit, $B(H \rightarrow J/\psi + \gamma) < 220 \times \text{SM prediction}$, with a part of the data collected by CMS during Run-2.

5. Expectations from HL-LHC

At High Luminosity upgrade of the LHC (HL-LHC) we expect to collect 3000/fb of data. The expected physics reach with this data set was investigated in Ref. [13]. Regarding the constraints on the H boson couplings to light quarks the results are summarized on Fig. 117 in [13]. At the time of

the preparation of the report (2018) it was expected to constrain H-charm coupling to 1.7 times the SM value, considering a global fit of all related data. Today (2022) it is expected that a comparable constraint will be reached from CMS VH(cc) search alone due to improvements of the analysis strategy [8]. This projection is based on the 1-jet topology analysis with some modifications. The details are provided in Fig. 50 of the additional material to Ref. [8], where the extrapolation of the sensitivity of the analysis to $H \rightarrow b\bar{b}$ and $H \rightarrow c\bar{c}$ decays at the HL-LHC is shown.

6. Conclusion

In this report I presented the analyses released by the CMS Collaboration before July 2022, aimed to constrain the coupling of the Higgs boson to the charm quark. The most sensitive expected limit is obtained with a direct search for $H \rightarrow c\bar{c}$ decay in VH production channel: $|\kappa_c| < 3.4$. Performing this analysis alone we expect to reach the limit of $|\kappa_c| < 1.7$ with HL-LHC data. Other channels and their global combination may help to improve this constraint even further. Standard model values of the H-charm coupling may be within reach in the next decades of the LHC operation.

References

- [1] ATLAS Collaboration, "Observation of a new particle in the search for the Standard Model Higgs boson with the ATLAS detector at the LHC", Phys. Lett. B 716 (2012) 1
- [2] CMS Collaboration, "Observation of a new boson at a mass of 125 GeV with the CMS experiment at the LHC", Phys. Lett. B 716 (2012) 30
- [3] CMS Collaboration, "Observation of a new boson with mass near 125 GeV in pp collisions at $\sqrt{s} = 7$ and 8 TeV", JHEP 06 (2013) 081
- [4] CMS Collaboration, "A portrait of the Higgs boson by the CMS experiment ten years after the discovery", Nature 607, 60–68 (2022)
- [5] CMS Collaboration, "Evidence for Higgs boson decay to a pair of muons", JHEP 01 (2021) 148
- [6] CMS Collaboration, "The CMS Experiment at the CERN LHC", JINST 3 (2008) S08004
- [7] CMS Collaboration, "Inclusive search for a boosted Higgs boson decaying to a charm quark pairs in proton-proton collisions at $\sqrt{s} = 13$ TeV", CMS-PAS-HIG-21-012
- [8] CMS Collaboration, "Search for Higgs boson decay to a charm quark-antiquark pair in proton-proton collisions at $\sqrt{s} = 13$ TeV", CMS-HIG-21-008, [arXiv:2205.05550]. Submitted to PRL. Additional material at: <http://cern.ch/go/Hdd9>
- [9] H. Qu and L. Gouskos, "Jet tagging via particle clouds", Phys. Rev. D 101, 056019
- [10] E. Bols et al, "Jet flavour classification using DeepJet", JINST 15 (2020) P12012
- [11] CMS Collaboration, "Measurement and interpretation of differential cross sections for Higgs boson production at $\sqrt{s} = 13$ TeV", Phys. Lett. B 792 (2019) 369
- [12] CMS Collaboration, "Search for rare decays of Z and Higgs bosons to J/ψ and a photon in proton-proton collisions at $\sqrt{s} = 13$ TeV", Eur. Phys. J. C 79, 94 (2019)
- [13] Cepeda, M. and others, "Report from Working Group 2: Higgs Physics at the HL-LHC and HE-LHC", CERN Yellow Rep. Monogr. 7 (2019) 221